Long-term MAX-DOAS Measurement of Aerosol and Trace Gases in the Environmental Research Station Schneefernerhaus (UFS), Germany

Zhuoru Wang*[1, 2], Nan Hao[1, 3], François Hendrick[4], Michel Van Roozendael[4], Udo Frieß[5], Robert Holla[6], Matthias Wiegner[7], Ka Lok Chan[7], Mark Wenig[7], Christian Schunk[8], Ludwig Ries[9], Klaus-Peter Heue[1], Adrian Doicu[1, 2], and Thomas Trautmann[1]

*e-mail: zhuoru.wang@dlr.de

(1) Remote Sensing Technology Institute (IMF), German Aerospace Center (DLR), Oberpfaffenhofen, Germany
(2) Faculty of Civil, Geo and Environmental Engineering (BGU), Technical University of Munich (TUM), Munich, Germany
(3) Now at: European Organisation for the Exploitation of Meteorological Satellites (EUMETSAT), Darmstadt, Germany
(4) Belgian Institute for Space Aeronomy (BIRA-IASB), Brussels, Belgium
(5) Institute of Environmental Physics (IUP), University of Heidelberg, Heidelberg, Germany
(6) German Meteorological Office (DWD), Hohenpeißenberg, Germany
(7) Meteorological Institute, Ludwig Maximilians University of Munich (LMU), Munich, Germany
(8) School of Life Sciences Weihenstephan (WZW), Technical University of Munich (TUM), Freising, Germany
(9) Global Atmosphere Watch, Federal Environmental Agency (UBA), Zugspitze, Germany

APPLIED REMOTE SENSING CLUSTER

Introduction

A MAX-DOAS Instrument has been working in the Environmental Research Station Schneefernerhaus (UFS) on Zugspitze, the highest mountain in Germany since 2011. The DSCDs (differential slant column densities) of O_4, NO_2, HCHO, and SO_2 etc. are measured, and the vertical profiles of tropospheric aerosol, NO_2, and HCHO, as well as the VCDs (vertical column densities) of stratospheric O_3 and NO_2 are retrieved.

Observation Site and Instrument

The Environmental Research Station Schneefernerhaus (Umwelt Forschungsstation Schneefernerhaus, UFS) is located under the summit of Zugspitze (2962 m), the highest mountain of Germany, at an altitude of 2650 m. This site is surrounded by the mountainous area of Alps, and the ambient air is mostly clean and unpolluted.

The MAX-DOAS instrument has been working since 2011. It consists of one telescope and two spectrometers.

Telescope location: on the terrace of the UFS
Telescope direction: southwards, towards the mountainous area of Alps
Vertical scanning sequence: 30°, 20°, 10°, 5°, 2°, 1°, -2°, 90° (scans only in vertical direction)
Spectral range: UV (320-478 nm before Feb 2016; 285-450 nm after May 2016), VIS (427-649 nm)

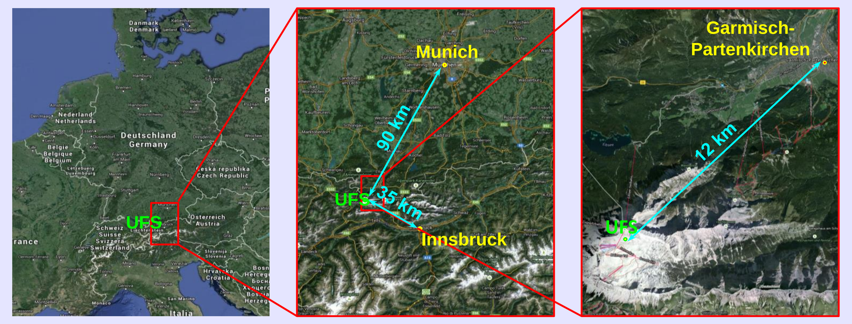

Fig. 1. Location of the UFS (47°25′00″N, 10°58′46″E)

Fig. 2. Surrounding view of the site

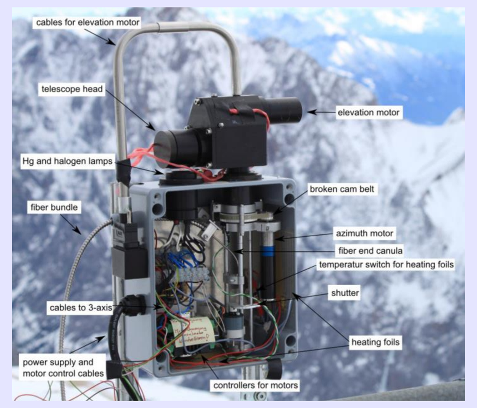

Fig. 3. Structure of the telescope (from Jurgschat, 2011)

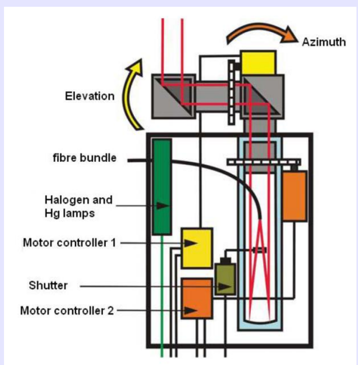

Fig. 4. Schematic view of the telescope (from Niebling, 2010)

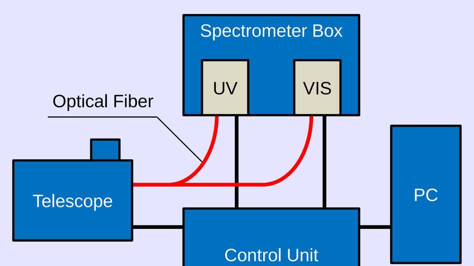

Fig. 5. Schematic view of the MAX-DOAS system

DSCD Calculation

Calculation tool: QDOAS (developed by BIRA-IASB)
Reference spectrum: for retrieving aerosol and trace gas profiles, the zenith spectrum of each scan; for calculating total VCDs, a fixed zenith spectrum measured at the noon in summer

Table 1. QDOAS settings for DSCD calculation

Band	UV			VIS				Reference
Data usage	profile retrieval					total VCD retrieval		
Destination	O_4	HCHO*	SO_2**	O_4	NO_2	O_3***	NO_2***	
Fitting window/nm	338-370	324.5-359	310-320	440-490	440-490	450-550	425-490	
Ring	×	×	×	×	×	×	×	Chance and Spurr (1997)
O_4	×	×	×	×	×	×	×	Hermans et al. (2011)
NO_2 294 K	×	×	×	×	×			Vandaele et al. (1998)
NO_2 220 K	×	×		×		×	×	Vandaele et al. (1998)
O_3 293K	×	×	×	×	×			Bogumil et al. (2003)
O_3 223K	×	×	×	×	×	×	×	Bogumil et al. (2003)
H_2O	×	×		×	×	×	×	HITRAN (2003)
HCHO	×	×	×					Meller and Moortgat (2000)
SO_2			×					Vandaele et al. (2009)
BrO			×					Fleischmann et al. (2004)
CHOCHO				×	×			Volkammer et al. (2005)
Polynomial	Order 4	Order 5	Order 5	Order 4	Order 4	Order 5	Order 5	

*: following the QA4EVC HCHO DSCD calculation setting **: only after 12.May.2016 ***: following the settings recommended by NDACC

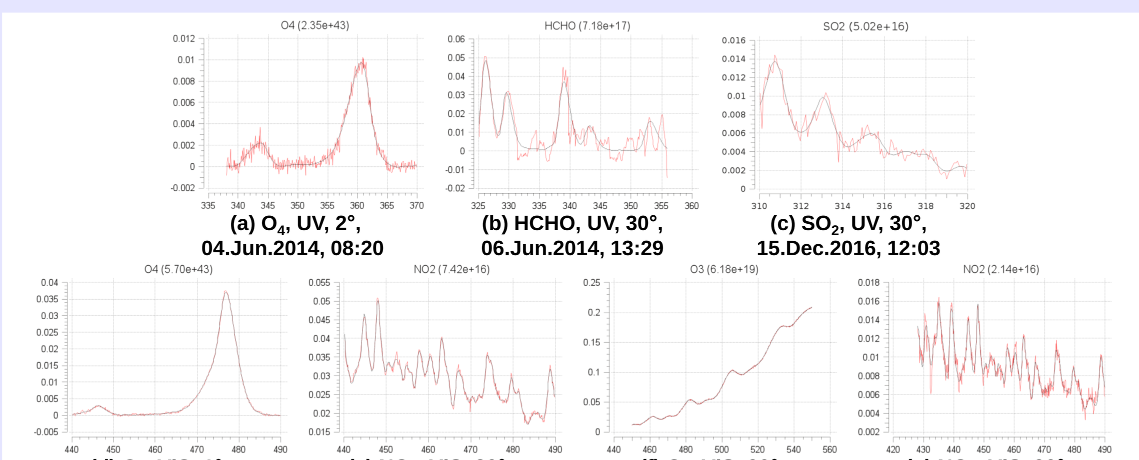

(a) O_4, UV, 2°, 04.Jun.2014, 08:20
(b) HCHO, UV, 30°, 06.Jun.2014, 13:29
(c) SO_2, UV, 30°, 15.Dec.2016, 12:03
(d) O_4, VIS, 1°, 22.Jun.2014, 06:11
(e) NO_2, VIS, 20°, 13.Jun.2014, 17:06
(f) O_3, VIS, 90°, 01.Nov.2014, 15:34
(g) NO_2, VIS, 90°, 01.Jan.2014, 15:19

Fig. 6. Examples of DOAS fitting (times refer to UTC)

Aerosol Profile Retrieval

The vertical profiles of aerosol are retrieved from the DSCDs of O_4 (oxygen dimmer).

Retrieval algorithm: bePRO (developed by BIRA-IASB, Clémer et al., 2010; Hendrick et al., 2014)
- Forward model: LIDORT radiative transfer model
- Retrieval method: Optimal estimation method (Rodgers, 2000)

Table 2. bePRO settings for aerosol profile retrieval

Band and wavelength		UV, 360 nm	VIS, 477 nm
Retrieval grid		2.65 - 5.05 km: 12 layers of 200 m thickness 5.05 - 6.05 km: 1 layer of 1000 m thickness	
Apriori profile		Fixed profile obtained from US Standard	
Surface albedo		0.03	0.05
Covariance matrix of a priori ($\mathbf{S}_a$)*	Apriori covariance scaling Factor (β)	0.35	0.1
	Apriori covariance correlation length	0.05	0.05

*: The diagonal element of $\mathbf{S}_a$ corresponding to the lowermost layer $\mathbf{S}_a(1, 1)$ is set equal to the square of β times the maximum partial aerosol optimal density (AOD) of the profile, and the other diagonal elements decrease linearly with altitude down to the product of the correlation length and $\mathbf{S}_a(1, 1)$ (Clémer et al., 2010; Franco et al., 2015).

Standard of valid results:
- Relative RMS (root mean square) between measured and simulated DSCDs <20%, and
- DFS (degrees of free signal) >1.0

Figs. 7 and 8 show the results of aerosol profile retrieval of a single scan in UV and VIS bands, respectively. Figs. 9 and 10 show the retrieval results of the entire day of 30.Aug.2015. That day was mostly clear, but there were some clouds in the afternoon.

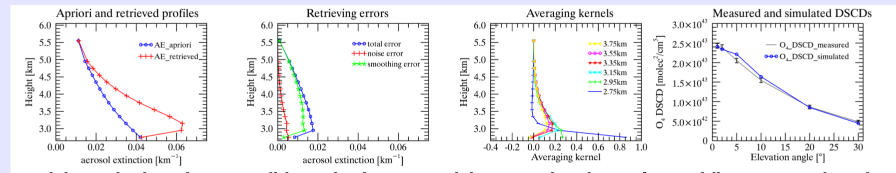

(a) a priori and retrieved profiles (b) retrieving errors (c) averaging kernels (DFS=1.684) (d) measured and simulated O_4 DSCDs

Fig. 7. Example of aerosol retrieval in UV band (30.Aug.2015 08:57 UTC)

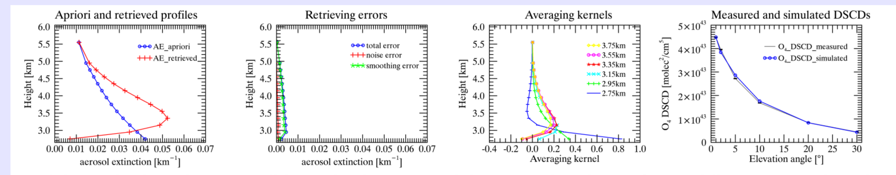

(a) a priori and retrieved profiles (b) retrieving errors (c) averaging kernels (DFS=1.942) (d) measured and simulated O_4 DSCDs

Fig. 8. Example of aerosol retrieval in VIS band (30.Aug.2015 08:57 UTC)

Figs. 11 and 12 show the average aerosol vertical profiles and the monthly average AOD. It can be seen that in both UV and VIS band, aerosol load is relatively high in summer. The difference between the results of the two bands might be explained by the different optical characteristics of aerosol at different wavelengths.

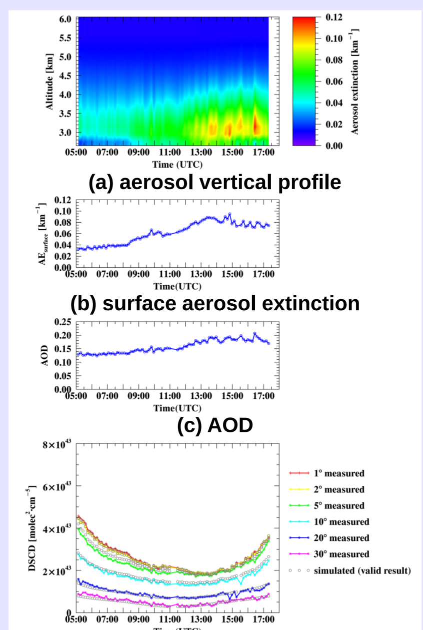

(a) aerosol vertical profile
(b) surface aerosol extinction
(c) AOD
(d) measured and simulated O_4 DSCDs

Fig. 9. Aerosol profile retrieval results of 30.Aug.2015 (UV)

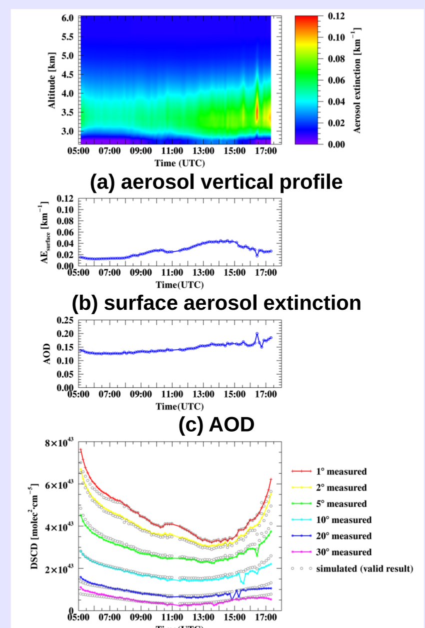

(a) aerosol vertical profile
(b) surface aerosol extinction
(c) AOD
(d) measured and simulated O_4 DSCDs

Fig. 10. Aerosol profile retrieval results of 30.Aug.2015 (VIS)

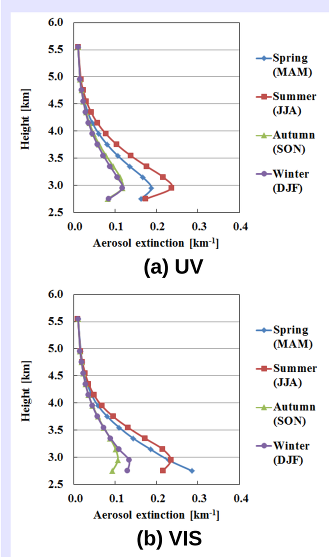

(a) UV
(b) VIS

Fig. 11. Average aerosol profiles in four seasons

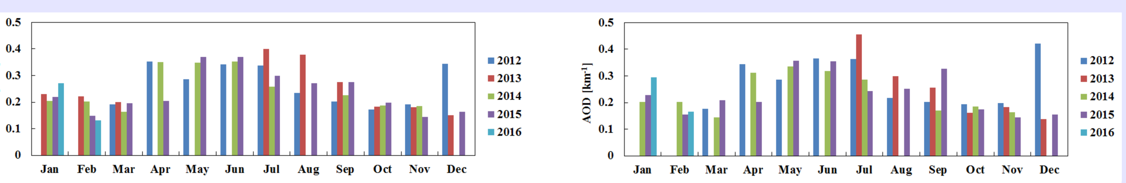

(a) UV (b) VIS

Fig. 12. Monthly average of AOD

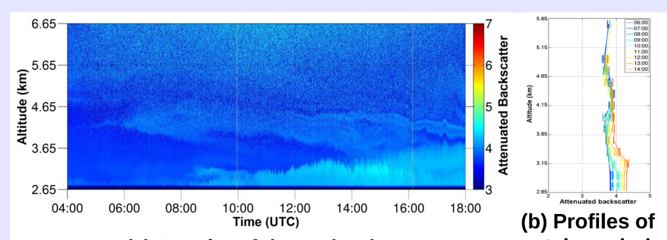

(a) Results of the entire day (b) Profiles of certain periods

Fig. 13. Ceilometer results of 30.Aug.2015

Comparison with ceilometer results: Fig. 13 shows the aerosol information of 30.Aug.2015 measured by a ceilometer at the UFS. The ceilometer results also show a increased aerosol load in the afternoon. (Note: the attenuated back-scattering factors measured by ceilo-meter are not directly comparable to aerosol extinction.)

Comparison with sun-photometer measurement: The AOD at 340 nm measured by a sun-photometer at the UFS at around 11:00 UTC on 30.Aug.215 is about 0.12. The AOD at 360 nm during that period retrieved from MAX-DOAS measurement is about 0.15.

Limitation of the study: Current radiative transfer models can only assume flat and homogeneous surfaces, cannot accurately simulate the radiative transfer above mountainous surfaces.

Trace Gas Profile Retrieval

The vertical profiles of trace gases are retrieved from the aerosol profiles and the DSCDs of the trace gases. The retrieval is also done with bePRO algorithm.

Table 3. bePRO settings for trace gas profile retrieval

Band, wavelength and trace gas species		UV, 360 nm, HCHO	VIS, 477 nm, NO_2
Retrieval grid		Same as aerosol retrieval	
Apriori profile		Fixed profile obtained from IMAGE model, change monthly	Fixed profile obtained from MOZART-2 model, change monthly
Surface albedo		0.03	0.05
Covariance matrix of a priori ($\mathbf{S}_a$)	Apriori covariance scaling Factor (β)	0.6	0.6
	Apriori covariance correlation length	0.2	0.2

Standard of valid results:
- Relative RMS between measured and simulated DSCDs <30%, and
- DFS >1.0

Figs. 14 and 15 show the results of HCHO and NO_2 retrieval of a single scan (the same scan as Figs. 7 and 8). Figs. 16 and 17 show the retrieval results of the entire day of 30.Aug.2015.

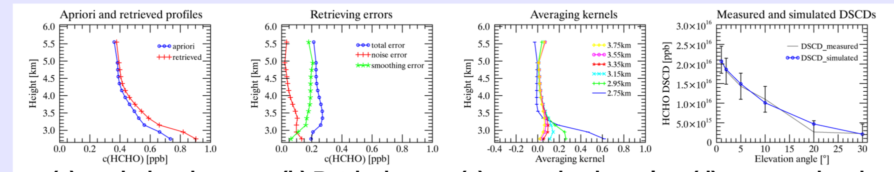

(a) a priori and retrieved profile (b) Retrieving errors (c) averaging kernels (DFS=1.291) (d) measured and simulated HCHO DSCDs

Fig. 14. Example of HCHO profile retrieval (UV, 30.Aug.2015 08:57 UTC)

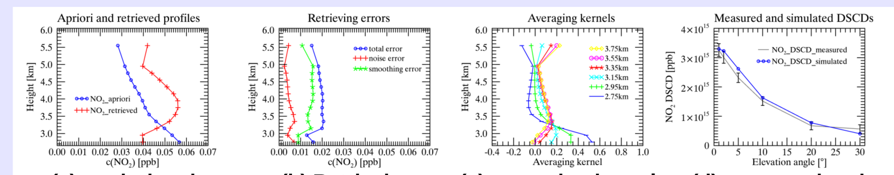

(a) a priori and retrieved profile (b) Retrieving errors (c) averaging kernels (DFS=1.992) (d) measured and simulated NO_2 DSCDs

Fig. 15. Example of NO_2 profile retrieval (VIS, 30.Aug.2015 08:57 UTC)

Figs. 18 and 19 show the average HCHO and NO_2 vertical profiles and the monthly average VCDs, respectively.

It can be seen that HCHO is highest in summer all along the year. This result agrees well with other studies, the enhancement of HCHO concentration in summer is caused by the stronger photo-chemical process in summer.

As for NO_2, it has 2 peaks in winter and summer. The peak in winter might be explained as the anthropogenic discharge; while in summer, it is noticeable in Fig. 18(b) that the concentration in higher layers is much higher than the other seasons, this might be due to the transmission between stratosphere and troposphere.

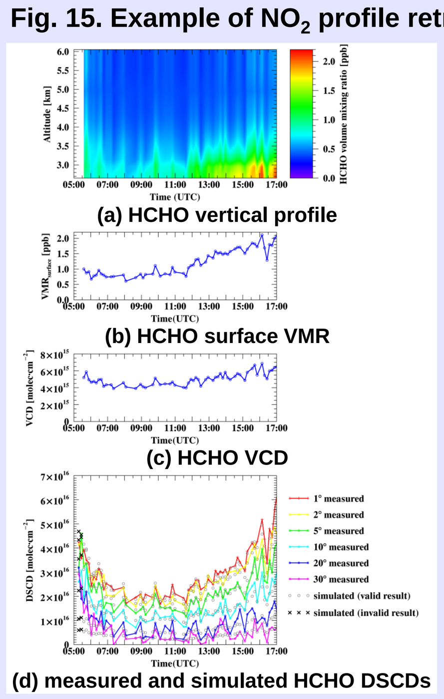

(a) HCHO vertical profile
(b) HCHO surface VMR
(c) HCHO VCD
(d) measured and simulated HCHO DSCDs

Fig. 16. HCHO profile retrieval results of 30.Aug.2015 (UV)

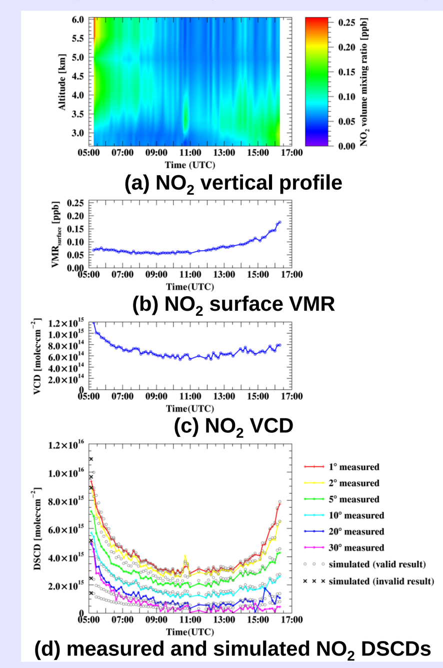

(a) NO_2 vertical profile
(b) NO_2 surface VMR
(c) NO_2 VCD
(d) measured and simulated NO_2 DSCDs

Fig. 17. NO_2 profile retrieval results of 30.Aug.2015 (VIS)

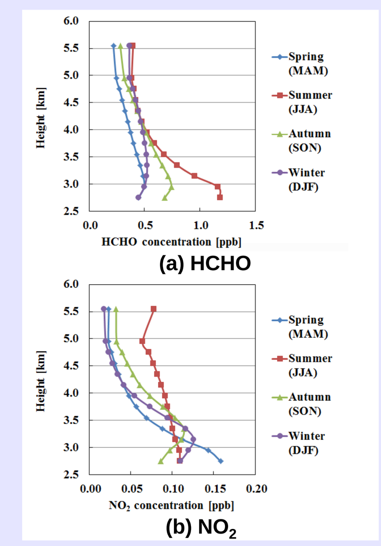

(a) HCHO
(b) NO_2

Fig. 18. Average trace gas profiles in four seasons

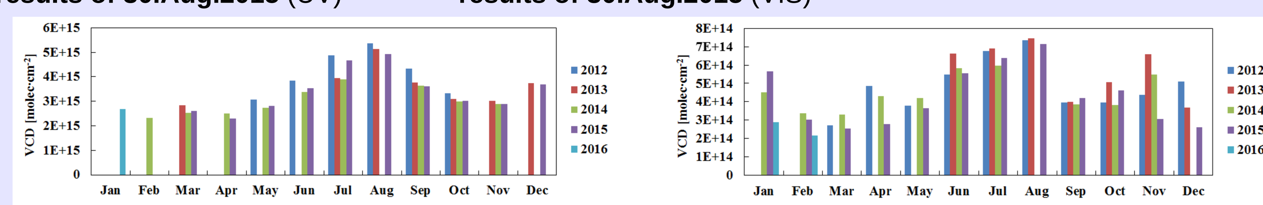

(a) HCHO (b) NO_2

Fig. 19. Monthly average VCD of HCHO and NO_2

Intercomparison with in-situ measurements: Figs. 20 and 21 show the comparison between the HCHO and NO_2 surface concentrations (average volume mixing ratio of 2.65-2.85 km for HCHO and 2.65-3.05 km for NO_2) retrieved from MAX-DOAS measurement and those measured by in-situ instruments (AeroLaser for HCHO and CRANOXII for NO_2) at the UFS. It can be seen that they agree well with each other.

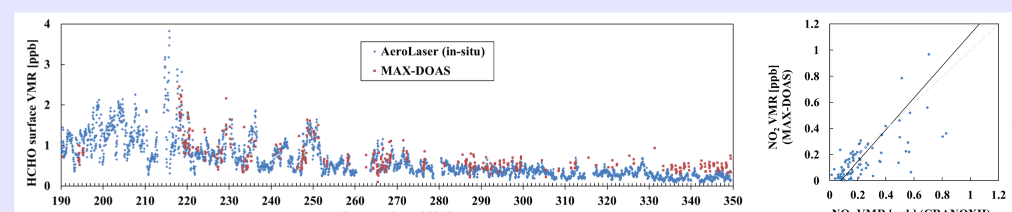

Linear regression equation:
$y = 0.6769x + 0.2543$
$R = 0.8122$

(a) time series of hourly average (b) x-y plot of daily average (values during daytime only)

Fig. 20. Intercomparison of HCHO surface concentrations measured by MAX-DOAS and AeroLaser

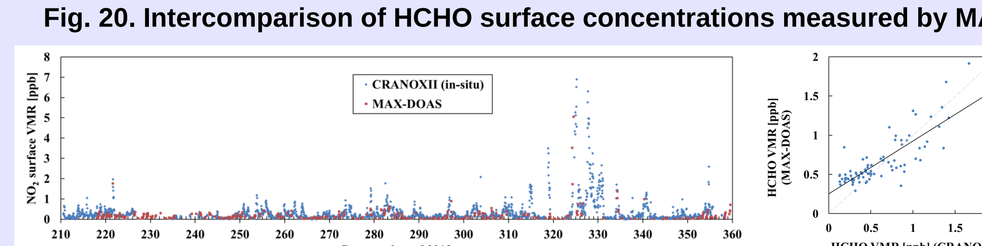

Linear regression equation:
$y = 1.2198x - 0.0948$
$R = 0.6632$
Note: there is one point (1.047, 3.416) lies out of the chart

(a) time series of hourly average (b) x-y plot of daily average (values during daytime only)

Fig. 21. Intercomparison of NO_2 surface concentrations measured by MAX-DOAS and CRANOXII

Total VCD of Trace Gases Retrieval

In this section, the DSCDs of O_3 and NO_2 are calculated from the zenith spectra measured during twilight hours (SZA=86-91°), with a fixed zenith spectrum measured in the noon of a summer day used as the reference spectrum. As the light path at noon is much shorter than that during twilight hours, the trace gas absorption in the reference spectrum can be neglected, so the DSCDs can be approximately seen as SCDs.

The AMFs (air mass factors) of O_3 and NO_2 are obtained from a look-up table developed by BIRA-IASB. The AMF data in the look-up table are calculated using the UVSPEC/DISORT radiative transfer model which includes a treatment of the multiple scattering in a pseudo-spherical geometry. The VCDs can then be derived by dividing the SCDs by the corresponding AMFs.

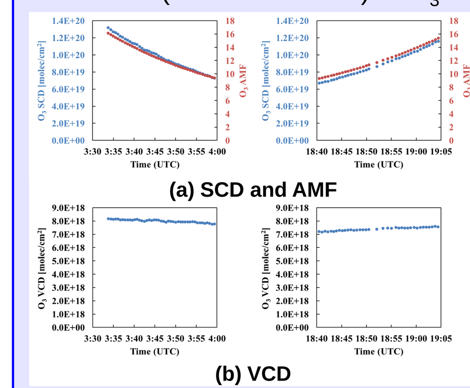

(a) SCD and AMF
(b) VCD

Fig. 22. Example of O_3 VCD measurement (03.Jul.2014)

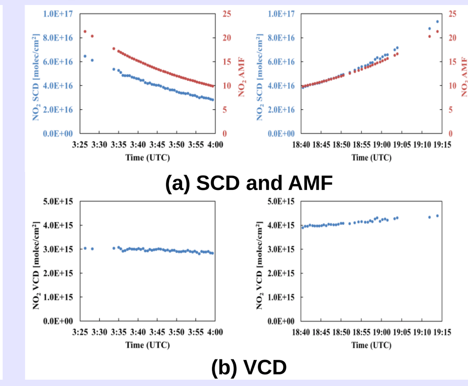

(a) SCD and AMF
(b) VCD

Fig. 23. Example of NO_2 VCD measurement (03.Jul.2014)

Figs. 22 and 23 show the SCDs, AMFs and calculated VCDs of one day. The stable VCD value suggests that the AMF is reasonable.

Figs. 24 and 25 compare the total VCDs of O_3 and NO_2 measured by MAX-DOAS and GOME-2A satellite. The satellite data are chosen from the data points within 150 km from the UFS. (The GOME-2A satellite is in a sun-synchronous orbit, it always pass over a place at 9:30 local time.) The data of the entire year of 2014 are shown in both time series and x-y plots.

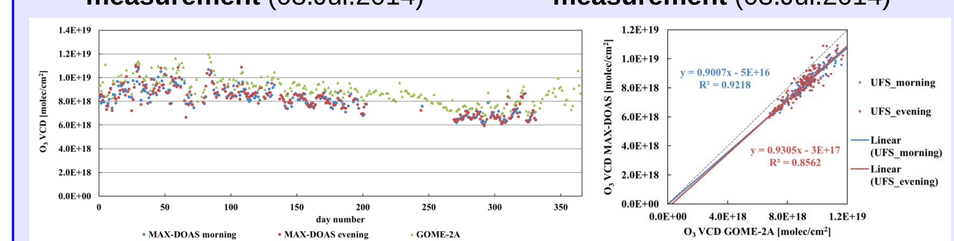

(a) time series (b) x-y plot

Fig. 24. Total O_3 VCDs measured by MAX-DOAS and GOME-2A (2014)

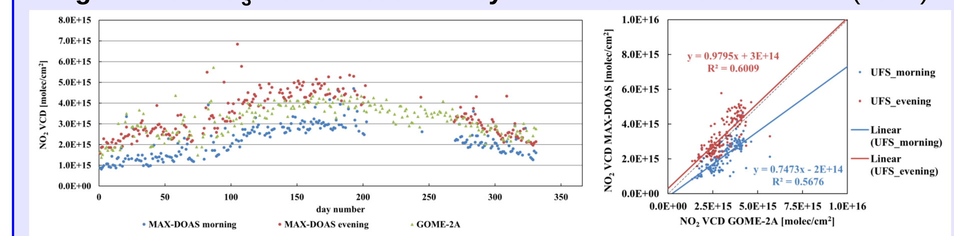

(a) time series (b) x-y plot

Fig. 25. Total NO_2 VCDs measured by MAX-DOAS and GOME-2A (2014)

It can be seen that the total VCDs of O_3 measured by MAX-DOAS and by GOME-2A satellite agree very well with each other. As for NO_2, the correlation is not so good as O_3, but still in a reasonable range. This might be explained that the total VCD of O_3 mainly exists in the Ozone layer in the stratosphere; but for NO_2, the existence in the troposphere also plays an important role. It is also noticeable that the VCDs of NO_2 measured by MAX-DOAS in the morning are lower than those measured in the evening, and the evening results agree much better with satellite data. This can be explained by the daily variation of NO_2. Moreover, the MAX-DOAS in the UFS measures almost only the free troposphere, while the satellite data cover some polluted areas.

Preliminary Results of SO_2 Measurement

From 12.May.2016 on, the former spectrometer of the UV band has been replaced by a new one which can cover the fitting window of SO_2.

Fig. 26 shows the daily average of SO_2 SCDs calculated from the zenith spectra in the noon (170°<SAA<190°), with the zenith spectrum measured at the noon of 20.Jun.2016 used as the reference spectrum.

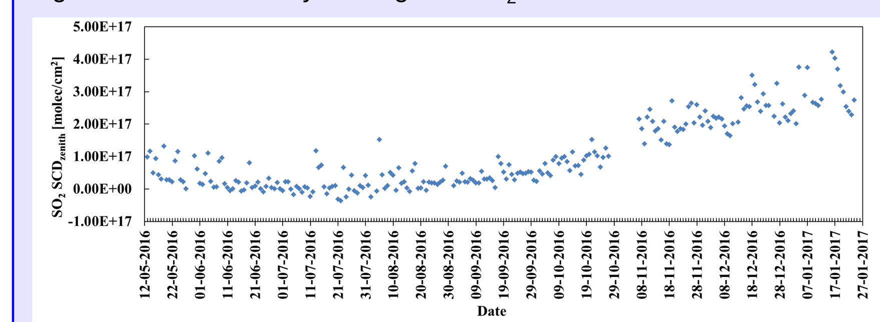

Fig. 26. Daily average of SO_2 SCDs of noon zenith spectra

Fig. 27 shows the daily average of tropospheric SO_2 VCD calculated with a simplified geometrical approach:

$$VCD_{trop} = \frac{DSCD}{\frac{1}{\sin(elev)} - 1}$$

Detailed explanation of this approach can be seen in (Brinksma et al., 2008) and (Jurgschat, 2011). In order to ensure the validity of such assumptions, the geometric VCDs of the highest two elevation angles (20° and 30°) of each scan are calculated and then compared, and only if the difference between the two results is below 30%, the result of this scan is retained.

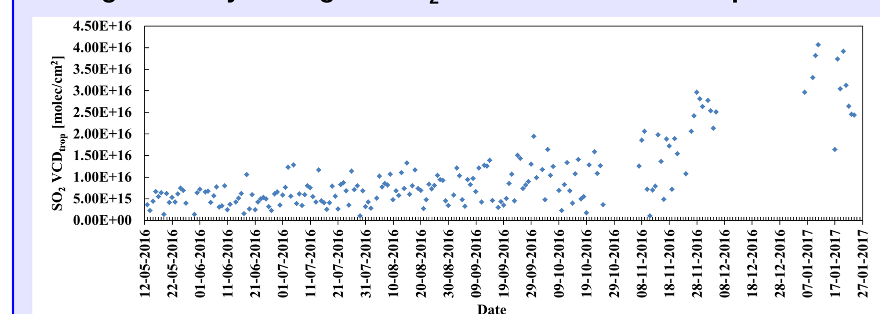

Fig. 27. Daily average of tropospheric SO_2 VCDs calculated with a simplified geometrical approach

It can be seen that both zenith SCD and tropospheric VCD of SO_2 are relatively high in winter. This can be explained by the higher SO_2 concentration in the atmosphere in winter due to the increased coal combustion. Moreover, the longer average light path due to the lower SZA in winter can also increases the SCD. No pollution episodes with significantly enhanced SO_2 VCD have been measured during this period.

Acknowledgement:
This work is funded by a DLR-DAAD (German Aerospace Center - German Academic Exchange Service) Fellowship Program.

References:

Brinksma, E. J., et al. (2008), The 2005 and 2006 DANDELIONS NO_2 and Aerosol Intercomparison Campaigns, J. Geophys. Res, vol. 113, D16S46, doi:10.1029/2007JD008808.

Clémer, K., et al. (2010), Multiple wavelength retrieval of tropospheric aerosol optical properties from MAXDOAS measurements in Beijing, Atmos. Meas. Tech., 3, 863-878, doi:10.5194/amt-3-863-2010.

Franco, B., et al. (2015), Retrievals of formaldehyde from ground-based FTIR and MAX-DOAS observations at the Jungfraujoch station and comparisons with GEOS-Chem and IMAGES model simulations, Atmos. Meas. Tech., 8, 1733-1756, doi:10.5194/amt-8-1733-2015.

Hendrick, F., et al. (2014), Four years of ground-based MAX-DOAS observations of HONO and NO_2 in the Beijing area, Atmos. Chem. Phys., 14, 765-781, doi:10.5194/acp-14-765-2014.

Jurgschat, M. (2011). Measurements of free-tropospheric trace gases with the MAX-DOAS method at the Environmental Research Station Schneefernerhaus. Master's thesis, University of Cologne.

Niebling, S. (2010). Langzeit-messungen von spurengasen und aerosolen mittels multi-axis-doas auf dem hohenpeißenberg. Master's thesis, University of Heidelberg.

Rodgers, C. D. (2000). Inverse methods for atmospheric sounding: theory and practice, Ser. Atmos. Oceanic Planet. Phys, vol. 2, F. W. Taylor, World, Sci., Hackensack, N.Y.

Schreier, S. F., et al. (2016), Estimates of free-tropospheric NO_2 and HCHO mixing ratios derived from high-altitude mountain MAX-DOAS observations at midlatitudes and in the tropics, Atmos. Chem. Phys., 16, 2803-2817, doi:10.5194/acp-16-2803-2016.

Wang, T., et al. (2014). Evaluation of tropospheric SO_2 retrieved from MAX-DOAS measurements in Xianghe, China, Atmos. Chem. Phys., 14, 11149-11164, doi: 10.5194/acp-14-11149-2014.